



HAL
open science

CO₂ Spontaneous Raman Scattering: an alternative thermometry for turbulent reactive flows

Florestan Guichard, Pascal Boubert, David Honoré, Armelle Cessou

► **To cite this version:**

Florestan Guichard, Pascal Boubert, David Honoré, Armelle Cessou. CO₂ Spontaneous Raman Scattering: an alternative thermometry for turbulent reactive flows. 19th International Symposium on the Application of Laser and Imaging Techniques to Fluid Mechanics, Aug 2018, Lisbon, Portugal. pp.16 - 19. hal-02381951

HAL Id: hal-02381951

<https://hal.science/hal-02381951v1>

Submitted on 16 Dec 2019

HAL is a multi-disciplinary open access archive for the deposit and dissemination of scientific research documents, whether they are published or not. The documents may come from teaching and research institutions in France or abroad, or from public or private research centers.

L'archive ouverte pluridisciplinaire **HAL**, est destinée au dépôt et à la diffusion de documents scientifiques de niveau recherche, publiés ou non, émanant des établissements d'enseignement et de recherche français ou étrangers, des laboratoires publics ou privés.

CO₂ Spontaneous Raman Scattering: an alternative thermometry for turbulent reactive flows

F. Guichard*, P. Boubert¹, D. Honoré¹, A. Cessou¹

¹: CORIA-UMR6614, Normandie Université, CNRS, INSA et Université de Rouen

Av de l'Université, 76800 Saint-Etienne-du-Rouvray

* Correspondent author: florestan.guichard@coria.fr

Keywords: CO₂, Spontaneous Raman Scattering, Temperature, Oxyfuel flame

ABSTRACT

Economic and ecological issues make necessary an in-depth study of combustion processes. Whether in-situ measurements of temperature are a key point to validate numerical combustion model, yet they still challenging in high temperature reactive flows. Previous studies have shown that non-intrusive thermometry method based on spectral fitting of N₂ Spontaneous Raman Scattering (SRS) was relevant to precisely characterize turbulent air flames. However, this technique may be less appropriate to study emerging processes such as oxyfuel combustion. The purpose of this paper is to demonstrate that spectral fitting of CO₂ SRS is a compelling alternative for temperature measurements in oxyfuel flames where N₂ is absent. Using a pure vibrational description of CO₂ SRS spectra, spectral fitting temperature measurements are made in several cases (heated gases, premixed laminar CH₄/air Bunsen flames) to assess the accuracy over a wide range of temperature, from 300 K to 2200 K. Measurements uncertainties depending on experimental conditions and CO₂ signal levels are also discussed. Finally, single-shot temperature profiles in the flame front of a premixed CH₄/O₂/CO₂ Bunsen flame shows an excellent agreement with simulation. This study opens a lot of prospects for future experimental studies of turbulent oxyfuel flames, especially in the objective of carbon capture and storage.

1. Introduction

The deep understanding of combustion phenomena, motivated by both economic and ecological issues, has justified the development of refined numerical simulation and more sophisticated optical diagnostics over the past years. Validation of theoretical and numerical combustion models requires accurate knowledge of temperature, species concentrations and their respective gradients. More specifically, temperature is a key parameter to study combustion processes, since it has a direct impact in a wide variety of factors, such as thermal efficiency, pollutant formation and product quality. Unfortunately, temperatures in flames are quite difficult to estimate. On one hand, classical thermometric tools such as thermocouple wires are no more appropriate due to the harshness of these hot and reactive media. On the other hand, there are a

few of non-intrusive temperature measurement techniques who are available and reliable over a wide range of temperature (between 300 K and 2500 K).

For many years, Spontaneous Raman Scattering (SRS) associated with Rayleigh Scattering has proven to be a compelling response to multi-scalar measurements needed in flames by simultaneous temperature and multispecies concentration measurements (Dibble and al. 1987, Bergmann and al. 1998, Barlow 2007, Fuest and al. 2011) even if its use remains seldom for flame investigation, especially turbulent, due to its signal weakness. In most Raman set-ups for combustion diagnostics, measurements consist in collecting simultaneously the strong Rayleigh scattering and SRS of major species, then using both to determine respectively temperature and number densities through an iterative procedure (“calibration” method and “hybrid” method). However, spontaneous Raman scattering alone contains enough information to determine temperature (Lapp and al. 1972), since the shape of SRS spectra is reflective of the rotational-vibrational energy distribution of the molecule probed. Thus by minimizing synthetic spectra with experimental spectra, temperatures can be extracted as long as the Signal Noise Ratio (SNR) is adequate.

This “spectral fitting” method is a powerful thermometric tool and has some advantages on the Rayleigh/Raman thermometry. First of all, no calibration is required since spectral fitting can directly be applied on normalized spectra, providing absolute temperature. Moreover, temperature is extracted from the spectrum of only one molecule. Thus, accuracy is independent of the uncertainties of other measurements. As soon as the SRS of the thermometric molecule is free of interferences, spectral fitting can be processed, even if the quality of some other parts of the full spectrum is badly deteriorated due to strong luminous interferences (e.g. flame emission, fluorescence, soot radiation...). Potential interferences that could nevertheless overlap the probed molecule SRS are easier to remove in the fitting method since spectra are acquired without on-chip binning. Last but not least, elastic light from wall reflections or from Mie scattering of potential droplets have a far less impact on pure SRS measurements than on Rayleigh scattering ones. In consequence, spectral fitting thermometry can also be used in complex burners, where Rayleigh thermometry is hard to use, if not impossible.

However, one drawback of the spectral fitting method is the weakness of the SRS signal, which is definitively lower than Rayleigh scattering. On top of that, if on-chip binning of SRS is very useful in calibration/hybrid method to improve the signal and minimize the readout noise, this operation is no more appropriate in the spectral fitting method. Since too noisy spectra induced high uncertainties on temperature and number density measurements, SRS spectral fitting was restricted for a long time to laminar flames studies where long exposure time are practicable to

balance the weakness of Raman radiation. However, the recent development of high energy excitation system and ultra-sensitive detectors makes now the spectral fitting method appropriate to the study of turbulent flames where high time and space resolutions are required (Ajrouche et al, 2014).

The accuracy of the spectral fitting thermometry relies mainly on the quality of the spectroscopic model used for the construction of the synthetic spectrum. This method is therefore limited to molecules whose spectroscopic data are available and sufficiently reliable. N_2 is a diatomic molecule whose spectroscopy has been deeply studied the last decades for SRS measurements. Thus, previous work have shown that the temperature provided by spectral fitting of N_2 SRS was highly accurate over a wide temperature range and uncertainties remained low for instantaneous measurements in flames (Ajrouche and al. 2014). Nevertheless, N_2 is not always present in abundance at any location in flames, and can be totally absent like in oxyfuel flames. The use of other species than N_2 for SRS thermometry is required especially in the purpose of providing reliable data for a better understanding of oxyfuel flame processes. In the objective of carbon capture and storage (CCS), CO_2 is the ideal molecule for this purpose, due to its high concentration in burnt gases, and also since oxygen is often diluted by CO_2 for limiting flame temperature. This means that CO_2 can be present both in fresh and burnt gases in sufficient quantity to be detectable and provide an acceptable Signal Noise Ratio (SNR) for instantaneous measurements in oxyfuel flame.

However, the polyatomic CO_2 SRS is ruled by a much more complex spectroscopy than the diatomic N_2 . Even if a lot of publications already described deeply CO_2 energy states, the computation of these numerous energy levels and transitions moments remains quite difficult for non-spectroscopists. Unfortunately, available databases for CO_2 at high temperature such as HITEMP (Rothman and al. 1992) or CDS (Tashkun and al. 2003) are designed for absorption or emission experiments and are not appropriate for Raman scattering. Last decade, CO_2 SRS rovibrational transitions have been computed by combustion experimentalists (Geyer 2005, Sepman and al. 2013), but the methodologies used (Blint and al. 1979, Finsterholzl 1982) are not be proved reliable for high temperature, resulting in some discrepancies between synthetic and experimental spectra in burnt gases.

Nevertheless, Lemus and al. (Lemus and al. 2014) have recently proposed a table of pure vibrational CO_2 SRS transitions computed through an algebraic method for combustion optical diagnostic purposes. Synthetic spectrum built with this table shows a good agreement with a high spectral resolution CO_2 SRS spectrum collected in burnt gases (Fernandez and al. 2006). The purpose of the present paper is to demonstrate that this recent and available database of pure

vibrational Raman transitions is appropriate for CO₂ SRS spectral fitting thermometry in oxyfuel flames and can be used for 1D single-shot measurements of temperature assorted with multispecies density number.

2. Experimental set-up

One of the distinguish features of SRS signal is its relative weakness, requiring the use of high energy laser excitation associated to appropriate sensitive detection system to reach high spatial and temporal resolution SRS measurements.

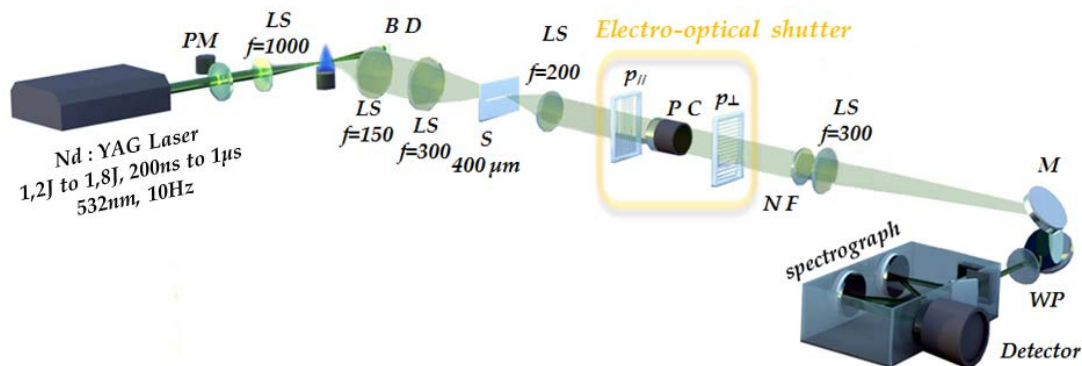


Fig. 1 Overview of the experimental set-up: S, slit; LS, Lens (AR coated @400-700nm) PC, Pockels Cell; P, Polarizer; BD, beam dump; PM, Power meter; NF, Notch filter (532 nm, FWHM 17 nm); WP, half-wave plate.

Figure 1 provides the overview of the experimental Raman setup. The excitation system consists in a high energy (about 1,8 J) laser pulses produced by the second harmonic (532 nm) of a Nd:YAG laser (Agilite, Continuum) at 10 Hz. The pulse duration is set at 1µs to stay under turbulence time scale and also to avoid optical breakdown due to excessive local irradiance. The laser beam is focused by a long focal-length lens ($f=1000$ mm) providing a 170 µm-thick probe volume almost constant along several millimeters.

The scattered light from a 3 mm-length probe volume is collected at 90° with a large solid angle by a first telescope of achromatic lenses. Then, a 400 µm-wide slit remove most of the flame emission from regions away from the probe volume. A second telescope of achromatic lenses and a periscope reimage the horizontal beam image for the 250 µm slit vertical entrance of an imaging spectrograph (IsoPlane SCT 320, 600g/mm gratings blazed at 500 nm, Princeton Instruments). An achromatic half-wave plate (AHWP10M-600, Thorlabs) is placed in front of the slit to get the best throughput of the spectrograph, which is sensitive to polarization direction of light. Finally, a Notch filter (NF03-532E, OD=6 at 532 nm, FWHM=17 nm, Semrock) is placed in the collimated region of the second telescope to reject elastic scattering lights, like Rayleigh and Mie scatterings, which are several orders of magnitude higher than SRS.

A full-frame back-illuminated CCD camera (Pixis 400B, 400 x 1340 pixels, Princeton Instruments) was placed at the focal plane of the imaging spectrograph to collect 1D single-shot SRS spectra. In the past, several detection systems have been compared for measurements by SRS (Ajrouche et al, 2016). Full-frame back-illuminated CCD camera appeared to be the most suitable both for its high quantum efficiency (>90%) and its low readout noise (<13e-), when associated to a fast gating system. Due to their full-frame architecture, such detectors without fast gating are continuously exposed during the readout time and the SRS signal can be completely drowned out by the flame emission. For this main reason, a fast electro-optical shutter has been developed to complete CORIA's experimental Raman setup (Ajrouche and al. 2015). This shutter is composed of two crossed polarizers (19WG-50, Quantum Technology) and a Pockels cell (LAP-50, KD*P, Quantum Technology). An HV generator (HVP-5LP, Quantum Technology) drives the Pockels cell crystal to get a 1,05 μ s gate width. More information and specifications about this original electro-optical shutter can be found in Ajrouche and al. (2015).

3. CO₂ SRS Spectra modeling

Measurements by spectral fitting rely mainly on the accuracy of the spectroscopic models used. For this reason, this method is often limited to diatomic molecules which are easier to describe than polyatomics. In contrast of diatomics which have only one vibrational mode (symmetrical stretching), the triatomic CO₂ has three different vibrational modes (symmetrical stretching, asymmetrical stretching and a doubly degenerated bending). Four quantum numbers (respectively ν_1 , ν_3 , ν_2 and l_2) are then required to describe all the vibrational energy levels of CO₂. Theoretically, only the symmetrical stretching is Raman active for a linear and symmetrical molecule with $\Delta\nu_1 = \pm 1$. Consequently, the SRS spectrum should be quite similar to the diatomic ones. However, in the specific case of carbon dioxide whose the first harmonic of ν_2 is almost equal half of the fundamental ν_1 , the bending mode is also Raman active with $\Delta\nu_2 = \pm 2$, because of Fermi resonance. These two selection rules associated to the combination of quantum numbers give rise to many allowed transitions, especially at high temperature as it can be seen in figure 2.

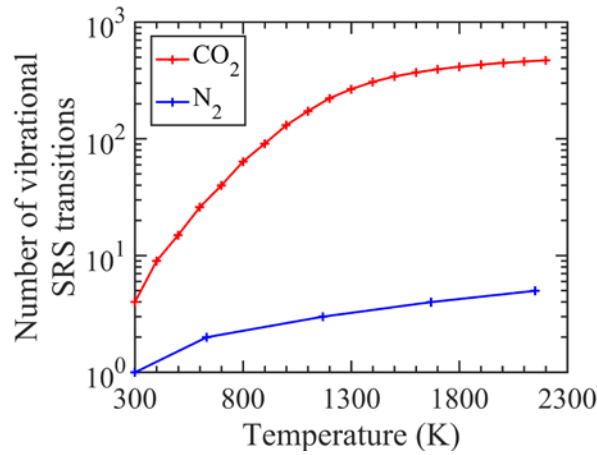


Fig. 2 Thermal evolution of the number of transitions required to get 99% of the total SRS cross-section of CO₂ and N₂ SRS

On this graph, the number of SRS transitions needed to reach 99% of the integrated cross section is plotted against temperature. The logarithmic scale highlights that this number of transitions is two orders of magnitude greater for CO₂ than for N₂ at high temperature.

The Fermi resonance also mixed the energy states satisfying $v_1+2v_2 = n$ (where n is an integer number), making the computation of energy levels, line positions and then line intensities much more complex than for diatomics. In this paper, CO₂ SRS spectra were modeled using a table recently released by Lemus and al. (2014) and specifically designed for combustion diagnostic. Their work is based on an original algebraic approach to keep a connection with configuration space and describe the CO₂ behavior with either local or normal coordinates. Their determination of the potential energy surface of CO₂, energy levels, polarizability derivatives and transitions moments shows good agreements with others works (Chedin 1979, Tejada and al. 1995, Zúñega and al. 2014). Finally, their simulation of a high resolution CO₂ spectrum in burnt gases shows results very close to experimental accuracy (Fernandez and al. 2006). More information can be found in their original papers where the methodology used is extensively detailed.

This spectroscopic table provides the positions line ν_{if} , the transitions moments M_{if} , energy ν_i and degeneracy g_i of the lower state, of 892 pure vibrational SRS transitions between 1100 and 1500 cm⁻¹, involving energy levels up to 15 000 cm⁻¹. The high number of transitions involved in this model should be enough to describe precisely the spectra of CO₂ up to 2200 K. Differential cross section of each line are computed with the following expression:

$$\left(\frac{\partial\sigma}{\partial\Omega}\right)_{i\rightarrow f} = \left(\frac{\pi}{\epsilon_0}\right)^2 \frac{(\nu_0+\nu_i-\nu_f)^4}{Z_{vib}(T)} g_i (M_{if})^2 \times \exp\left(\frac{-h\nu_i}{k_b T}\right) \quad (1)$$

Where ϵ_0 is the permittivity of vacuum, h the Planck constant, k_b the Boltzmann constant, ν_0 the wavenumber of the exciting radiation, ν_i and ν_f respectively the lower and the upper levels involved in the transition, and $Z_{vib}(T)$ the vibrational partition function.

Synthetic spectra are built by convoluting all the individual Raman peaks (defined by a Raman shift and a cross section) with an instrumental function. The figure 4 shows an example of synthetic CO₂ SRS built at 2000 K with a 0,001 nm Gaussian linewidth. It can be noticed that the large number of very close vibrational transitions causes slight overlapping, even at this high spectral resolution.

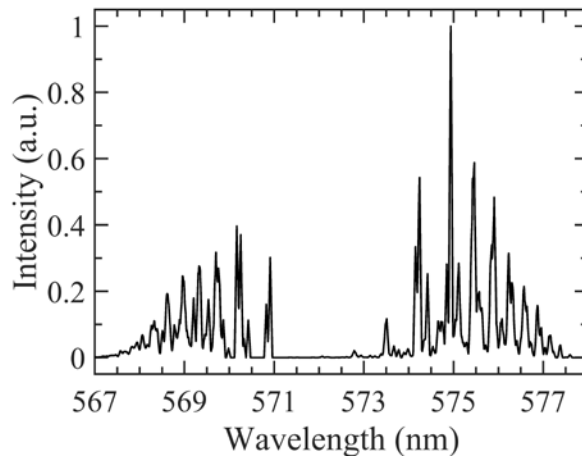


Fig. 3 High resolution synthetic CO₂ SRS spectrum (T= 2000 K ; linewidth=0,001 nm)

A pure vibrational description of the CO₂ Raman spectra is relevant in this study. For N₂, a quite strong rotational-vibrational interaction leads to a shift $d\nu_J$ of the Q-branches with rotational quantum number J increasing such as:

$$d\nu_J = -\alpha_e J(J + 1) \quad (2)$$

However, this effect which causes a smearing of the vibrational transitions of N₂ is definitely smaller for CO₂ ($\alpha_e=0,018$ cm⁻¹ for N₂ and $\alpha_e=0,0028$ cm⁻¹ for CO₂). Thus, all the CO₂ Q-branches reside very close to one another and overlap, leading to sharp and strong individual lines which can be considered as pure vibrational transitions (Eckbreth 1996). This assumption is also very attractive in spectral fitting method since the number of transitions to fit is significantly reduced.

4. Results and discussion

To ensure that synthetic vibrational spectra is reliable, experimental CO₂ SRS were acquired with the previous described Raman set-up. Several cases were studied in order to cover a wide range of temperatures and densities. To make CO₂ SRS measurements at low temperature, cold gases were heated using an 8kW electrical heater (Sureheat JET, OSRAM Sylvania). The target

temperature T_{thermo} was reached thanks to a control loop using a K-type thermocouple at the outlet of the heater. The maximum temperatures extended to about 1000 K. 25%/75% CO₂-air gas mixture, provided by RMS flowmeters were thus heated. Flow rates were always above 60slpm to avoid the overheating of equipment. The heater was placed vertically and the measurements were made to the closest position from the exit to avoid dilution with ambient air. To study CO₂ SRS at higher temperature (around 2100 K), measurements were made in the burnt gases of a premixed laminar stoichiometric CH₄-air flame of a Bunsen burner ($Re \approx 1000$). 400 instantaneous CO₂ experimental spectra were thus averaged and compared with a synthetic spectrum minimized at T_{thermo} in hot gases and T_{N_2} in burnt gases. This later was determined through the spectral fitting of N₂ SRS, whose accurate thermometry in flames had been shown in previous works with the procedure proposed (Lo and al. 2012, Ajrouche and al. 2016). Both CO₂ and N₂ SRS synthetic spectra were computed using an instrumental function obtained in-situ by fitting simulation spectra with measurements of N₂ SRS in ambient air and using a gaussian function as approximation. Figure 4 shows the comparison between a 400-single shots averaged spectra and the minimized synthetic spectrum of CO₂ SRS spectra measured in hot gases ($T_{\text{thermo}}=1004$ K) (left) and burnt gases ($T_{N_2}=2138$ K) (right).

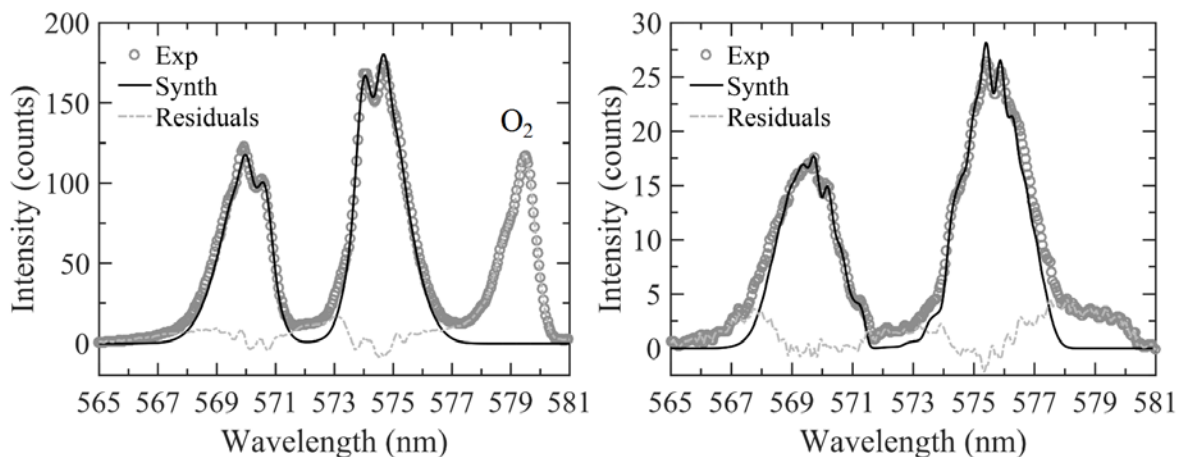


Fig.4 Comparison between average experimental CO₂ spectra and synthetic minimized at T_{N_2} : in hot gases (left) in burnt gases (right)

It can be noticed that most of the individual vibrational transitions seen previously in figure 3 actually overlap because of the large width of the instrumental function (0,67 nm). This quite low spectral resolution required for multi-scalar measurement may degrade the thermal sensitivity of the CO₂ and be problematic to measure temperature. However, in both cases, the two resulting broad parts of CO₂ Raman spectra are well reproduced by the model in respect of their relative intensities and positions. This can be seen on the smallness of residuals that are globally below 10%. Nevertheless, a substantial difference with the experimental data can be observed on

the wings of the CO₂ SRS spectra. This is assumed to be some marks of rovibrational Raman transitions (O, S, P and R-branches) occurring in this range of wavelength, which are not taken into account by the pure vibrational model used here.

The impact of the little discrepancies and the low resolution on the accuracy of T_{CO_2} is assessed. First, the minimization procedure has been carried out on the full CO₂ SRS spectra. In hot gases, from 300 K to 1000 K, the CO₂ temperature was systematically overestimated, leading to a maximal error of 53 K at 1000 K. As shown of figure 6, this quite acceptable accuracy of about 95% drops of to 85% in burnt gases, where the CO₂ temperature is overestimated at 2441 K, much higher than the adiabatic flame temperature. Figure 5 shows that this overestimation is due to the tendency of the minimization process to reduce the difference between the synthetic spectra and the experimental spectra in the wing regions where the discrepancies are observed.

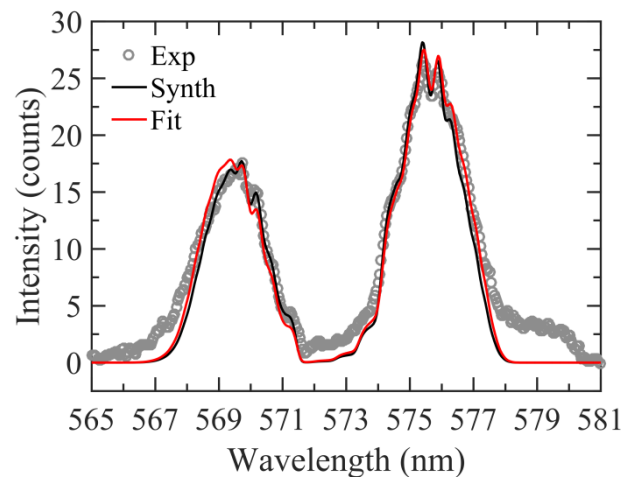


Fig.5 - Comparison between synthetic ($T=2138$ K), experimental and fitted ($T=2441$ K) CO₂ spectra in burnt gases. To improve accuracy, new borders for the minimization were then fixed to reduce the influence of the CO₂ ro-vibrational wings. The minimization procedure was carried out only on some parts of the CO₂ spectra (568.75 nm - 572 nm and 574 nm - 575.5 nm) to offer the best thermal sensitivity and to be relevant for a wide range of temperature. In this way, the minimization of the reduced CO₂ SRS spectra increased the accuracy of T_{CO_2} in burnt gases from 85% to more than 97% ($T_{\text{CO}_2}= 2151$ K with $T_{\text{N}_2}= 2134$ K at the same location of the methane/air flame). The systematic overestimation of temperature in hot gases was also reduced by 40% leading to a maximum error of 33 K with T_{thermo} at 1004 K. A compilation of averaged measurement of T_{CO_2} compared with T_{thermo} and T_{N_2} in figure 6 shows that the accuracy of the temperature determination is very satisfactory from 300 K to 2100 K, showing that the measurement is enough sensitive and accurate despite the low spectral resolution.

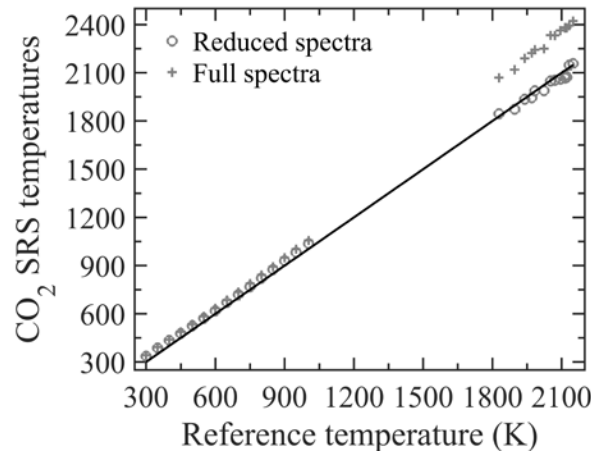


Fig.6 - Comparison of T_{CO_2} with T_{thermo} (between 300 K and 1000 K) and T_{N_2} (between 1800 K and 2200 K)

After defining this appropriate post-processing procedure from analysis of averaged spectra, the accuracy and uncertainties of single-shot measurements have now to be determined in the purpose of measurement in turbulent flames. 400 single-shot CO_2 temperature measurements are collected and then post-processed. The minimization procedure was applied to each single-shot spectrum, with the previously fixed borders. In hot gases, CO_2 SRS temperature is about $1037 \text{ K} \pm 48 \text{ K}$, which is quite close to the one found with N_2 SRS ($1017 \text{ K} \pm 50 \text{ K}$) and with the thermocouple measurement (1004 K). These relatively low uncertainties are mainly due to the high SNR (greater than 30) of the CO_2 SRS in this 25% CO_2 / 75% air gas mixture

To see if these uncertainties are still low at high temperature, minimization was carried out on single-shot spectra taken along the burnt gases of the stoichiometric flame. Two temperature measurements were performed simultaneously from N_2 and CO_2 spectra, the averaged values of single-shot temperatures and their standard deviation are displayed in figure 7.

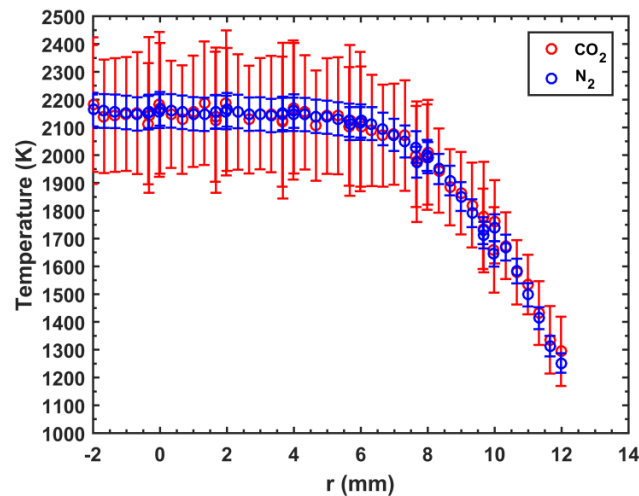


Fig.7 - N_2 and CO_2 temperature averaged profiles obtained from single-shot SRS spectra in burnt gases of methane-air flame

On this figure, an excellent agreement can be observed between the 400 averaged single-shot T_{CO_2} and T_{N_2} at each location in the burnt gases. In the hottest area (2134 K), the difference between T_{CO_2} and T_{N_2} does not exceed 40K, and is most of the time around 15 K, which leads to an accuracy greater than 98%. Nevertheless, the CO_2 temperature is affected by greater uncertainties ($2133 \text{ K} \pm 240 \text{ K}$) than for N_2 temperature ($2147 \text{ K} \pm 55 \text{ K}$). These more important uncertainties can be explained by the density difference of the two species. About 8% of CO_2 and 70% of N_2 can be found in the burnt gases of this stoichiometric CH_4 /air flame, leading to SNR of 7 and 37 respectively. This quite low CO_2 SNR has an impact during the minimization procedure where the more noisy single-shot CO_2 spectra (as can be seen in figure 8) result finally in a greater dispersion of the temperature measurements.

Finally, single-shot CO_2 temperature measurements are accurate and reliable from 300 K to 2200 K but are impacted by greater uncertainties in stoichiometric CH_4 /air flame because of low SNR. Therefore, T_{N_2} should be prioritized in the specific case of air flame where the SNR of N_2 is much higher than the one of CO_2 . Nevertheless, the absence of N_2 in oxyfuel flame applications justified the use of CO_2 SRS for thermometry.

This potential is now checked by 1D single-shot SRS measurements made in the burnt gases of a CO_2 diluted rich CH_4/O_2 Bunsen flame ($\phi=1.18$). The high volume fraction of carbon dioxide (56,4%) in this configuration provides a higher signal level of CO_2 than in the case of the previous CH_4 /air flame. Single-shot spectra acquired in the burnt gases of both flames are compared in fig.8 to highlight the effect of SNR on the quality of the spectra to minimize. Thus, the high SNR (equal to 37) of CO_2 SRS in the oxyfuel flame leads to moderate uncertainties on temperature ($2142 \text{ K} \pm 79 \text{ K}$) while the lower SNR (equal to 7) of CO_2 SRS in the air flame increases significantly these uncertainties ($2133 \text{ K} \pm 240 \text{ K}$).

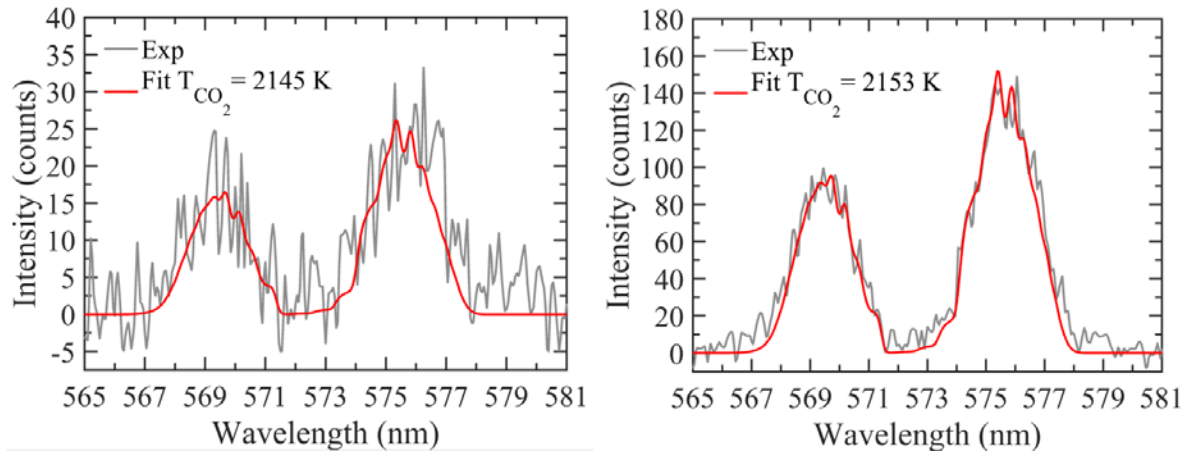


Fig.8 – Comparison of two single-shot spectra in the burnt gases of CH₄/air flame (left) and CH₄/O₂/CO₂ flame (right)

Moreover, in this configuration, CO₂ molecules are present both in fresh and burnt gases, making possible temperature measurement across the flame front. 400 single-shot CO₂ temperature profiles were then acquired 12mm from the bottom of the conical flame with the same spatial resolution as previously (330μm). However, in order to prevent any spatial averaging effect, 400 additional single-shot CO₂ temperature profiles were also acquired at a higher spatial resolution (200μm), by increasing the binning of the camera resulting in 13 simultaneous probe volumes. Since the laser beam did not cross the flame front perpendicularly, experimental profiles were corrected from the angle effect assuming that the tangential temperature gradients were negligible at the height probed, far from the flame tip and burner lip. Moreover, since the flame front was oscillating during the experiment, all the single-shot profiles are translated to superpose the position of the maximal gradient. This latter is localized for each single-shot profile by an interpolation with a complementary error function (erfc). Once the effect of the flame motion and angle effect are removed, single-shot thermal profile for both resolutions can be displayed and compared with simulation in figure 9. Modeling calculation was performed with Cantera software, assuming a 1D freely propagating laminar flame in the same initial conditions and using the GRI-Mech 3.0 chemical mechanism.

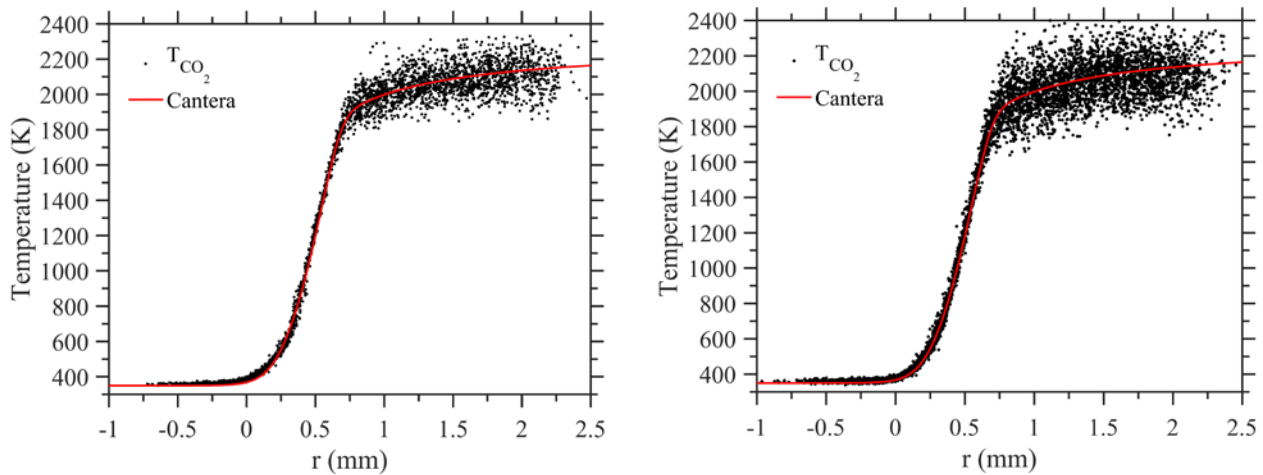


Fig.9 - Distribution of single-shot CO_2 temperatures across the $\text{CH}_4/\text{O}_2/\text{CO}_2$ flame front with $330\mu\text{m}$ resolution (left) and $200\mu\text{m}$ resolution (right)

On these instantaneous profiles, it can be noticed that all single-shot profiles are very close to the one provided by simulation. Fresh and burnt gases areas are clearly identified and the sharp temperature gradient is well described for both spatial resolutions. This proves the reliability and the accuracy of T_{CO_2} from 300 K to 2200 K, i.e. on the full range of temperature of this oxyfuel flame. Measurements' accuracy is identical for both resolutions, showing that no spatial averaging effect is occurring in this experiment. However, a greater dispersion of temperature measurements can be observed for the 200 μm profile. These higher uncertainties come from the reduced SNR due to the higher spatial resolution. In the burnt gases, CO_2 SNR with 330 μm resolution is around 37, leading to 3,7% of uncertainties on T_{CO_2} . With 200 μm resolution, CO_2 SNR drops off to 22 and increases the uncertainties to 5,6%. Nonetheless, these uncertainties around 5% are still well appropriate to describe reliable single-shot temperature profile, especially with such high spatial resolution.

5. Conclusion

The present work proposes CO_2 ramanography for absolute temperature measurements for the study of oxyfuel flames. The method used in this paper is based on the spectral fitting of experimental spectra with new CO_2 SRS transitions recently computed by spectroscopists for combustion diagnostic. It has been shown that a pure vibrational description of SRS CO_2 is finally appropriate to measure temperature accurately, despite a discrepancy on the wings of the spectra. CO_2 Raman SRS have shown a satisfactory thermal sensitivity over a wide range of temperature (between 300 K and 2200 K) even with a low spectral resolution for multi-scalar measurements. A CO_2 -diluted oxyfuel flame front has then been fully and precisely measured by single-shot measurements. The high energy (1,8 J) of the excitation system associated to the great sensitivity of the detection system leads to moderate uncertainties (around 5% in the burnt

gases) in single-shot measurement for a high spatial resolution (200 μm). This study opens prospects for the analysis of turbulent oxyfuel flames by simultaneous 1D measurements of temperature and concentrations of major species.

Acknowledgements

This work is funded by the BIOENGINE project. The project BIOENGINE is co-financed by the European Union with the European regional development fund (ERDF) and by the Normandy Regional Council. This work was also supported by the EXFIDIS project with the financial support of the French National Research Agency (ANR-13-BS09-0014). The PhD fellowship of F. Guichard is supported by Normandy Regional Council.

References

- H. Ajrouche, A. Lo, P. Vervisch, A. Cessou, (2014), 1D single-shot thermometry in flames by Spontaneous Raman Scattering through a fast electro-optical shutter, 17th Int. Symp. Appl. Laser Tech. to Fluid Mech. Lisbon, Port
- H. Ajrouche, A. Lo, P. Vervisch, A. Cessou, (2015) Assessment of a fast electro-optical shutter for 1D spontaneous Raman scattering in flames Measurement Science and Technology, 26 075501
- H. Ajrouche, A. Lo, P. Vervisch, A. Cessou, (2016) Detector Assessment for 1D Single-Shot Spontaneous Raman Scattering for Temperature and Multi-Species Measurements in Flames 18th Int. Symp. Appl. Laser Tech. to Fluid Mech. Lisbon, Port
- R.S. Barlow (2007) Laser diagnostics and their interplay with computations to understand turbulent combustion, Proceedings of the Combustion Institute, 31, 49-75
- V. Bergmann, W. Meier, D. Wolff, W. Stricker (1998) Application of spontaneous Raman and Rayleigh scattering and 2D LIF for the characterization of a turbulent $\text{CH}_4/\text{H}_2/\text{N}_2$ jet diffusion flame Appl. Phys. B, 66 489-502
- R. J. Blint, J. H. Bechtel and D. A. Stephenson (1979) Carbon dioxide concentration and temperature in flames by Raman spectroscopy J. Quant. Spectrosc. Radiat. Transfer Vol. 23, pp. 89-94
- A. Chedin (1979) The Carbon Dioxide Molecule: Potential, Spectroscopic, and Molecular Constants from its infrared Spectrum, J. Mol. Spect., 76 430-491
- R.W. Dibble, A.R. Masri, R.W. Bilger, (1987) The spontaneous Raman scattering technique applied to nonpremixed flames of methane Combust. Flame, 67 189-206.
- A.C. Eckbreth (1996) Laser Diagnostics for Combustion Temperature and Species, CRC Press,

- H. Finsterholzl (1982) Raman Spectra of Carbon Dioxide and Its Isotopic Variants in the Fermi Resonance Region, *Ber. Bunsenges. Phys. Chem.* 86, 797-805
- F. Fuest, R.S. Barlow, D. Geyer, F. Seffrin, A Dreizler (2011) A hybrid method for data evaluation in 1D Raman spectroscopy, *Proceeding of the Combustion Institute*, 33 815-822
- D. Geyer (2005) 1D-Raman/Rayleigh Experiments in a Turbulent Opposed-Jet, PhD thesis, ISBN 3-18- 353306-5, Technical University of Darmstadt, Germany,
- M. Lapp, L.M. Goldman, C.M. Penney (1972) Raman Scattering from flames, *Science*, 175 1112
- R. Lemus, M. Sanchez-Castellanos, F. Pérez-Bernal, J.M. Fernandez, M. Carjaval (2014), Simulation of the Raman spectra of CO₂: Bridging the gap between algebraic models and experimental spectra *J. Chem. Phys.* 141
- A. Lo, G. Cléon, P. Vervisch, A. Cessou, (2012), Spontaneous Raman scattering: a useful tool for investigating the afterglow of nanosecond scale discharges in air, *Applied Physics B: Lasers and Optics*, 107 229-242
- J.M. Fernandez, A. Punge, G. Tejada, S. Montero (2006) Quantitative diagnostics of a methane/air mini-flame by Raman spectroscopy, *J. Raman Spectroscop*, 37 175-182
- L.S. Rothman, R.L. Hawkins, R.B. Wattson and R.R. Gamache, (1992), Energy levels, intensities and linewidths of atmospheric carbon dioxide bands, *J. Quant. Spectrosc. Radiat. Transfer.* 48 537-566
- A.V. Sepman, V.V. Toro, A.V. Mokhov, H.B. Levinsky, (2013), Determination of temperature and concentration of main components in flames by fitting measured Raman spectra, *Appl. Phys. B*, 112 35-47
- S.A. Tashkun, V.I. Perevalov, J-L. Teffo, A.D. Bykov, N.N. Lavrentieva (2003), CDS-1000 the high-temperature carbon dioxide spectroscopic databank, *J. Quant. Spectrosc. Radiat. Transfer.* 82 165-196
- G. Tejada, B. Maté and S. Montero, (1995), Overtone Raman spectrum and molecular polarizability surface of CO₂, *J. Chem. Phys.* 103 568-576
- J. Zúñiga, J. Cerezo, A. Bastida and A. Requena, (2014) Rovibrational energies, partition functions and equilibrium fractionation of the CO₂ isotopologues, *J. Quant. Spectrosc. Radiat. Transfer.* 147 233-251